CEBAF
DESIGN OVERVIEW AND PROJECT STATUS

Christoph Leemann

Continuous Electron Beam Accelerator Facility*
12000 Jefferson Avenue, Newport News, Virginia 23606

Introduction

The Continuous Electron Beam Accelerator Facility (CEBAF) will be an electron accelerator facility for nuclear physics research providing continuous beams with energies up to at least 4 GeV and currents up to 200 μA. The Vogt Subcommittee of the Nuclear Science Advisory Committee has stated the physics objective of this new accelerator:

> *The search for new nuclear degrees of freedom and the relationship of nucleon-meson degrees of freedom to quark-gluon degrees of freedom in nuclei is one of the most challenging and fundamental questions of physics.*[1]

CEBAF's purpose thus is to study the structure of the nuclear many-body system, its quark substructure, and the strong and electroweak interactions governing the behavior of nuclear matter. This requires electron beams of sufficient

- energy to provide the kinematic flexibility required to study the transition region,
- intensity (current) to allow precise measurement of relatively small electromagnetic cross sections,
- duty factor to allow coincidence experiments,
- beam quality to allow high-resolution experiments.

This combination of characteristics—high energy, high current, high duty factor, high beam quality—makes CEBAF a unique tool for nuclear physics research.

The need for such an accelerator was first formulated in 1976 by a panel of the National Academy of Science[2] (G. Friedlander, Chairman); subsequent panels[3,4,5,6] reaffirmed the need for and refined the requirements of such an accelerator. In winter 1982/83 the NSAC Panel on Electron Accelerator Facilities[7] (D. A. Bromley, Chairman) received and evaluated five competing proposals at the requests of NSF and DOE. DOE adopted the NSAC-endorsed panel recommendation to accept the proposal by SURA (Southeastern Universities Research Association), developed under the the leadership of Professors James McCarthy and Richard York of the University of Virginia.

* Supported by DOE Contract #DE-AC05-84ER4015

This proposal originally foresaw a 2 GeV, S-band, disc-loaded, pulsed, room temperature linac that would reach 4 GeV by one "head to tail" beam recirculation, and cw beams at the experimental end stations through the use of a stretcher ring. An internal technology review[8] conducted by the author as well as extensive external review[9,10,11] established in summer and fall of 1985 that rf superconductivity had reached a maturity that allowed large-scale application, as demonstrated by research progress in the US, Western Europe, and Japan. For reasons to be outlined below, the 1500 MHz structure developed at Cornell University's Newman Laboratory of Nuclear Studies[12] was determined to be most suitable for the needs of the CEBAF project. DOE proposed the project in this form to Congress for construction start in FY '87.

Design Rationale, Performance Objectives, Concept and Fundamental Choices

A true cw device is the approach of choice to produce a high quality continuous beam; low peak current for a given average current facilitates the achievement of low emittance, and continuously operating rf systems can be controlled more precisely in both phase and amplitude, thereby leading to smaller energy spread and lesser variations of average energy. The conceptually simplest approach would be a straight linac, and the most mature technology that of room temperature rf structures operating in the range of 1500 to 3000 MHz. This approach, however, leads to excessive power consumption and/or high capital cost. At high duty factor, particularly in cw operation, copper cavities lose their gradient advantage achievable in short pulse operation: at a gradient of 3 MV/m power dissipation in excess of 100 kW/m not only leads to excessive power demand ($\gtrsim$ 100 MW for GeV range beams) but also limits achievable gradients below those of superconducting structures, where 5 MV/m can be viewed as a conservative specification. At this gradient, assuming cavity Q-values in the 10^9 range and cryogenic plant efficiencies of $\sim 10^{-3}$, total power dissipation translates into wall plug power of a few kW/m. This lowers power consumption into a more realistic realm, but even then a straightforward superconducting linac of 4 GeV would not yet be a cost-effective approach, with regard to both operating and initial capital expense. This last optimizing step is accomplished through recirculation, i.e., the repeated passing of the beam through the same accelerating section.

The CEBAF Recirculating Linac Concept

Figure 1 illustrates schematically the CEBAF recirculating linac concept. Four-pass recirculation was chosen as being close to the cost minimum and of acceptable complexity. Total accelerator circumference is minimized by splitting the acceleration structure in two equal segments located in the straight sections of the racetrack configuration. Each segment contains 100 m active length, in the form of 200 five-cell 1497-MHz CEBAF-Cornell type superconducting cavities, thus providing 0.5 GeV energy gain per segment at a gradient of 5 MV/m. Eight cavities are combined in each cryomodule, each of which is connected to its neighbor by a warm

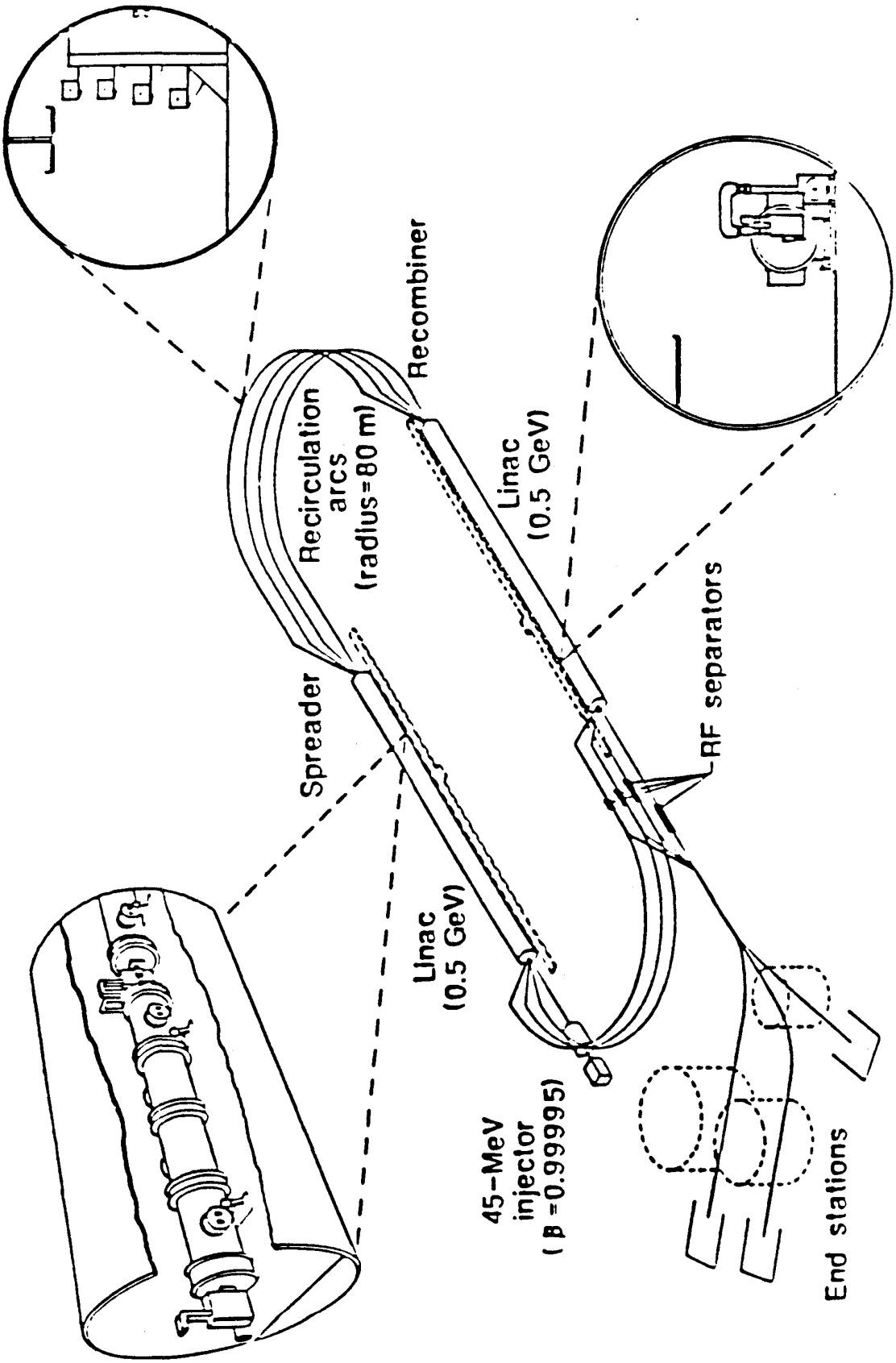

Figure 1. Schematic of CEBAF superconducting, 4-pass recirculating linac.

section containing beam vacuum pipe, vacuum equipment and magnetic elements (quadrupoles and steering dipoles) to focus and guide the beam (Fig. 2).

The beam transport lines connecting the two linac segments are achromatic and isochronous, provide matching in all phase space coordinates, and are designed with generous bend radii and strong focusing to minimize quantum excitation.

The entire machine is operated in true electron linac mode, i.e., with the particle bunches "riding the crest" of the sinusoidal rf wave shape without longitudinal focusing, relying on the extreme relativistic motion of the electrons. At the nominal injection energy of 45 MeV, indeed, total phase slip (with respect to a reference particle moving at $\beta \equiv 1$) is less than 2°, through four passes, most of which occurs in the first half of the first pass through the first segment.

The multi-user beam distribution system has three key elements: the injector, the availability of physically separated beams of different energies in the recirculation transport lines, and the use of rf-separators (deflecting cavities). The injector creates three interspersed bunch trains, $k + 3N, k = 0, 1, 2$, and $N = 0, 1, 2, 3...$, where bunches with different k can have different bunch charges, i.e., currents. The rf-separators deflect the beam and septum magnets allow the amplification of this separation and the extraction from the machine. At an operating frequency of 1000 MHz for the rf-separators and 1500 MHz for the rf system, the separator phases are independent of N and amount to ϕ_0, $\phi_0 + 240°, \phi_0 + 120°$ for bunch trains $k = 0, 1, 2$ respectively. Of particular usefulness are the initial phases $\phi_0 = 0$, leading to 0°, 240°, 120° resulting in a "straight," "left," "right" distribution (e. g., for distributing beams of equal energy to three end stations), and $\phi_0 = 90°$, leading to 90°, 330°, 210° resulting in a "one right," "two left" separation sequence.

Beam Performance Objectives

Beams of the order of 200 μA current and energies up to 4 GeV were established in 1982 by the nuclear physics community[5] as the beam performance objective of the CEBAF project. After changing technology and design concept, stringent demands for beam quality can be met (a key advantage) and the high user multiplicity is naturally "built in."

Performance objectives are:

Energy E [GeV]	$0.5 \leq E \leq 4.0(6.0)$
Beam current [μA]	$I \leq 200$
Duty factor	cw
Emittance	$\epsilon \simeq 2 \cdot 10^{-9}$ m
Momentum spread	$\sigma_E/E = 2.5 \cdot 10^{-5}$
User multiplicity	3 with up to 3 different (although correlated) energies

The energy of 4.0 GeV is a baseline specification; based on cavity prototyping experience, we anticipate sufficient enough energy gain per pass to reach 6.0 GeV,

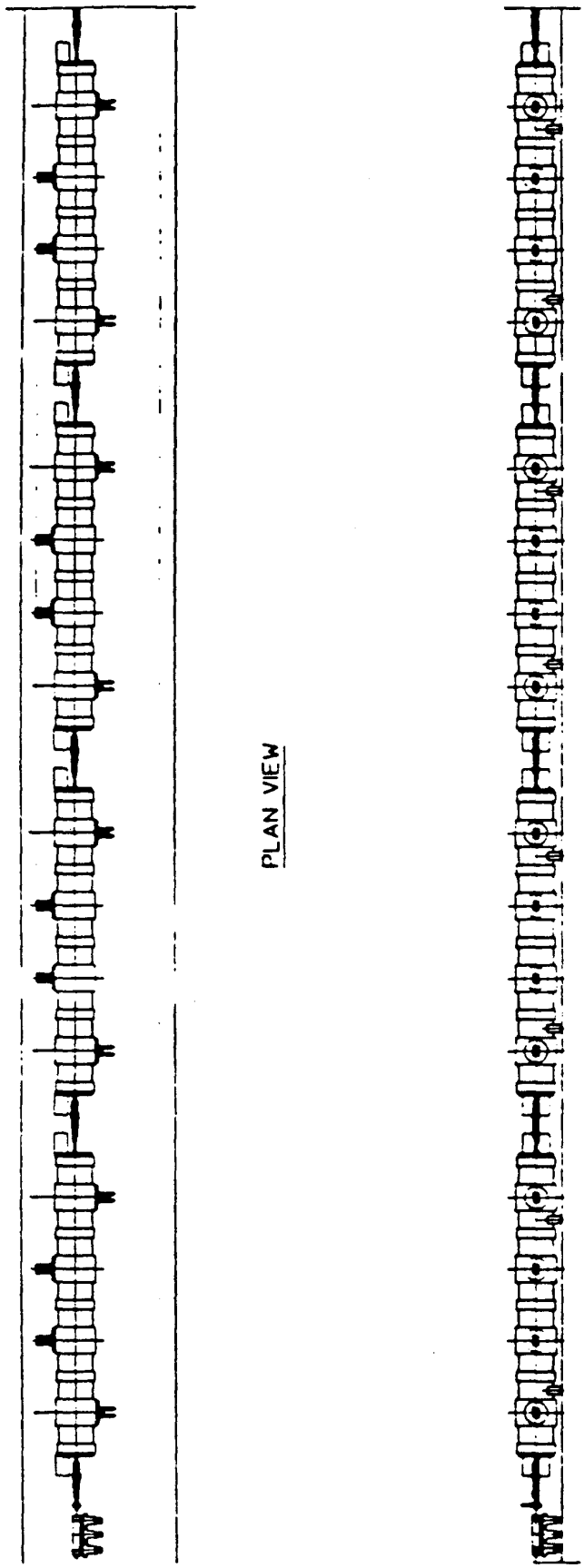

Figure 2. Elevation and plan view of superconducting accelerating structure. Visible are cryomodules, each containing eight cavities, fed alternately from left and right, and the intervening warm sections.

and all elements are thus designed so as not to prevent this. The 200-μA total output current is distributed in controllable ratios between the three end stations. The emittance is unnormalized and refers to the "full beam" size, i.e., $\sigma_x^2 = \frac{1}{4}\epsilon_x\beta_x$. The value of $\epsilon = 2 \cdot 10^{-9}$ m at 1 GeV is equivalent to $\epsilon_N \simeq 10^{-6}$ m in "storage ring parlance," (i.e., $\sigma_x = \epsilon_{N,x}\gamma\beta_x$). Due to various emittance degrading effects we do not quote the normalized emittance: $\epsilon < 2 \cdot 10^{-9}$ m at $E > 1$ GeV is not precluded but not necessarily guaranteed.

Fundamental Design Choices

Among the fundamental decisions in the design of a large recirculating linac such as CEBAF are the choice of rf frequency (which furthermore involves a choice of approximate operating temperature), the number of recirculations, and the average radius of the recirculating arcs.

Given the high-technology nature of the superconducting cavities, the long development time for each of today's successful examples, and the potential schedule impact of departures from proven design, the choice of frequency furthermore implies the choice of a very specific design. CEBAF's adoption of the 1500 MHz Cornell design thus rests first on the availability of a proven design, developed by a group in reasonable proximity, willing to support a neophyte laboratory to the point of not only participating in an industrial prototyping program but effectively joining the CEBAF team. Second, with the envisaged rf-separator extraction scheme, 1500 MHz approaches the lower limit acceptable for the nuclear physics user from the point of view of optimal time structure of the beam. Lower frequency, of course, has great attraction with lower impedances or wakefields, scaling as f^{m+2} with frequency for m-pole fields, and alternate extraction patterns have at least conceptually been devised. Nevertheless, with the modest peak current but high duty factor requirements of nuclear physics, 1500 MHz remains a most rational choice from the prime user's point of view.

The number of recirculations is the result of an optimizing procedure that not only involves costs, which early in the design may not be known to sufficient precision, but also judgment with regard to complexity and technical risk. Many variations of this approach indicate a broad cost minimum between three to six passes, four being the ultimate choice.

The size of the arcs is determined by the maximum energy and the expected beam quality, i.e., by how much degradation due to synchrotron radiation is tolerated. We decided that single-cell results with gradients in excess of 20 MV/m justified the assumption that within a decade, 20 MV/m multicell cavities will very likely be available. Such cavities would allow upgrade of CEBAF's energy to 16 GeV, or more generally to somewhere between 10 and 20 GeV. The arcs were therefore laid out, loosely packed with dipoles, such that by installation of a more tightly packed lattice with larger magnetic radius, beams in that energy range could be transported with satisfactory degradation of emittance and momentum spread.

The CEBAF Design: Systems Highlights

Table 1 summarizes the CEBAF accelerator parameters.

Injector

The injector provides a high-quality electron beam that is sufficiently relativistic (nominal 45 MeV) to stay in phase with the rf and the recirculating electron beams in the first half of the linac. The bunching, capture, and initial acceleration (up to 0.6 MeV) regions are modeled after proven injector designs [13,14]. This beam is then further bunched and accelerated to just over 5 MeV in two five-cell superconducting cavities in a short cryostat, and then accelerated in two full-sized cryomodules to the required 45 MeV before injection into the linac. The entire injector has been modeled with PARMELA, a two-dimensional particle simulation code that calculates phase and radial properties, including space charge effects, for an electron beam. Calculations indicate that a bunch of less than 1° phase angle and 20 keV full width should be obtained at the exit of the injector[15]. The injector enclosure has been designed to accommodate two electron guns to provide both polarized and unpolarized beams.

Acceleration Systems: Cavities, Cryogenic System, and RF System

The accelerating cavities are five-cell, 1497 MHz, elliptical cavities developed at Cornell University (Fig. 3). The cavities operate in the π mode, and have a fundamental coupler on the beam line at one end and an HOM (higher order modes) coupler on the beam line at the other. The elliptical cavity shape yields low peak surface electric fields, a good chemical rinsing geometry, and good mechanical rigidity. The HOM coupler has two waveguides for extraction of HOMs. HOM Q's are typically in the range of $500 \lesssim Q_{\mathrm{HOM}} \lesssim 170{,}000$, which represents five orders of magnitude of damping.

The Cornell cavity was adopted for CEBAF for four important reasons: suitable frequency, gradients in excess of 5 MV/m in laboratory and beam tests, damping of HOMs, and technical maturity, i.e., readiness for industrial prototyping.

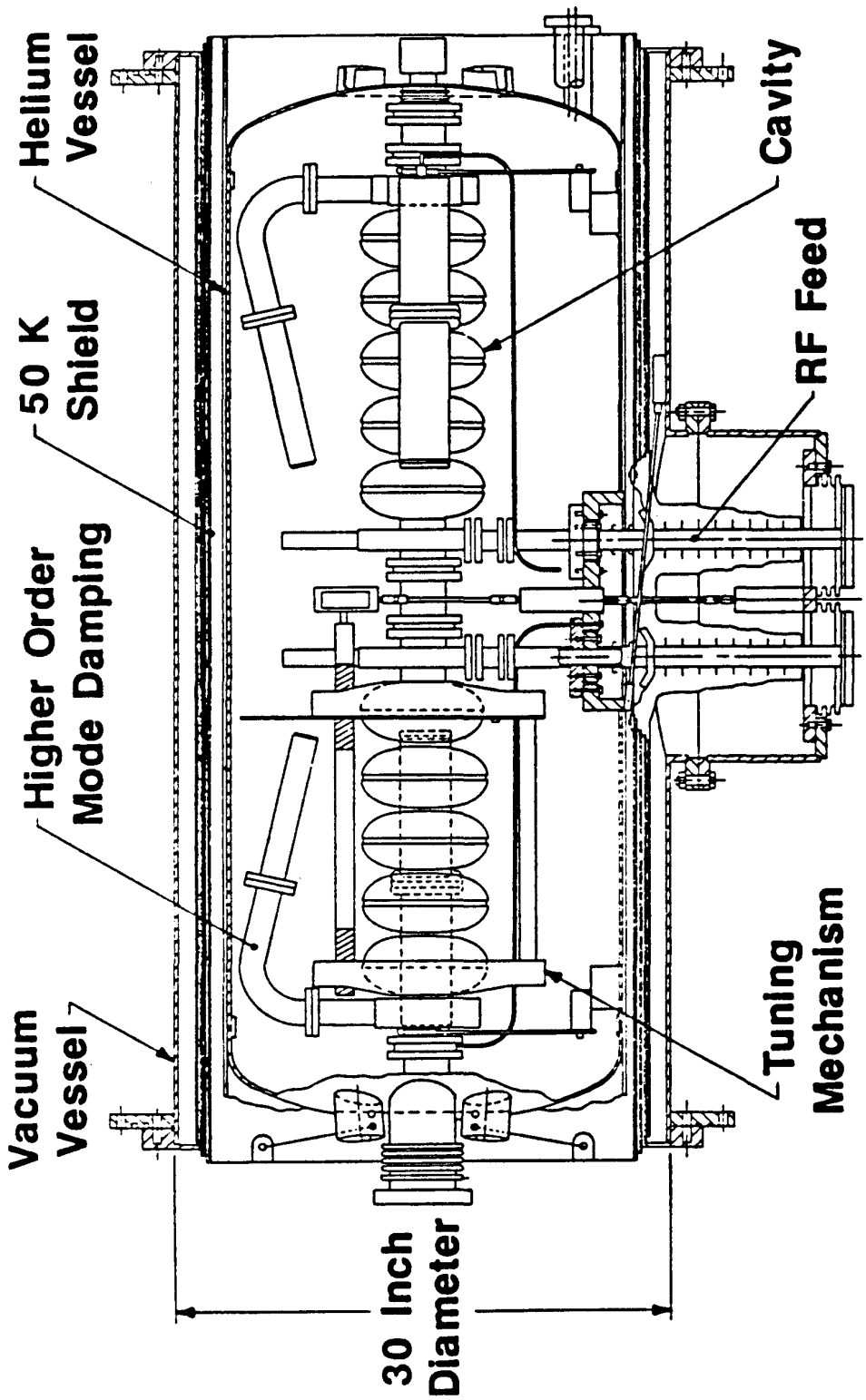

Figure 3. CEBAF-Cornell cavity pair.

Table 1
Design Parameter List

CEBAF Superconducting Radio-Frequency CW Linac	
Beam characteristics	
electron energy E [GeV]	$0.5 \leq E \leq 4.0$ (6.0)
average current [μA]	200
transverse emittance (95%, 1 GeV)[m]	2×10^{-9}
energy spread (95%)	1×10^{-4}
duty factor	100%
simultaneous beams	3
simultaneous energies	≤ 3
Linac parameters	
concept	superconducting cw recirculating linac
number of passes	4
number of linac segments	2
segment length [m]	235
maximum energy gain per pass [GeV]	1.0
recirculation time per pass [μs]	4.2
focusing	FODO
phase advance per cell (pass 1)	120°
half-cell length [m]	9.6
cavities per half-cell	8
half-cells per segment	25
vacuum (before cooldown)[Torr]	10^{-9}
Cavity parameters	
type	superconducting
frequency [MHz]	1497
electric length (m)	0.5
shunt impedance (r/Q)[Ω/m]	960.0
design gradient (MV/m)	5.0
design Q_0 at 2 K, 5 MV/m	2.4×10^9
typical HOM Q_{external}	10^3 to 10^5
clear aperture [mm]	70
transverse HOM Z''/Q[Ω/m^3]	$\leq 16.4 \times 10^4$
loaded Q (fundamental mode)	6.6×10^6

RF system	
number of klystrons	418
klystron power rating [kW]	5.0
phase control	$<1°$
gradient regulation	$<10^{-4}$
Injector parameters	
gun energy [MeV]	0.10
injection energy [MeV]	45
average current [μA]	200
transverse emittance (at 0.1 MeV)[mm·mr]	1
longitudinal emittance [keV · degrees)	$<15\ \pi$
bunch length [degrees] at 45 MeV	<1.0
pulse capability [μs]	0.05 to 10
Recirculation arc beam lines	
number	7
magnetic radii[m]	11.5 to 28.6
phase advance per period	$2\ \pi(5/4)$
periods per arc	4
Cryogenic system	
total rf load (2.0 K)[W]	2510
total heat load (2.0 K)[W]	3310
system capacity (2.0 K)[W]	4800
total heat load (45 K)[W]	8000

The operating temperature was selected on the basis of a cost optimization study. Liquid helium refrigeration systems become more expensive (capital and operating costs) as their design temperature decreases. Yet rf heat losses in the cavities increase exponentially with temperature. For CEBAF the optimum is around 2.0 K, as indicated in Fig. 4.

The cryogenic system for CEBAF consists of a 5 kW central helium refrigerator and a transfer line system to supply 2.2 K, 2.8 atm helium to the cavity cryostats, 45 K helium at 4.0 atm to the radiation shields, and 4.5 K helium at 2.8 atm to the superconducting magnetic spectrometers in the experimental halls. Both the 2.2 K and the 4.5 K helium are expanded by Joule-Thompson (JT) valves in the cryostats, yielding 2.0 K at 0.031 atm and 4.4 K at 1.2 atm, respectively. The central helium refrigerator is located in the center of the CEBAF racetrack with the transfer lines located in the linac tunnels.

The CEBAF rf system consists of 418 individual rf amplifier chains (Fig. 5). Each superconducting cavity is phase-locked to the master drive reference line to

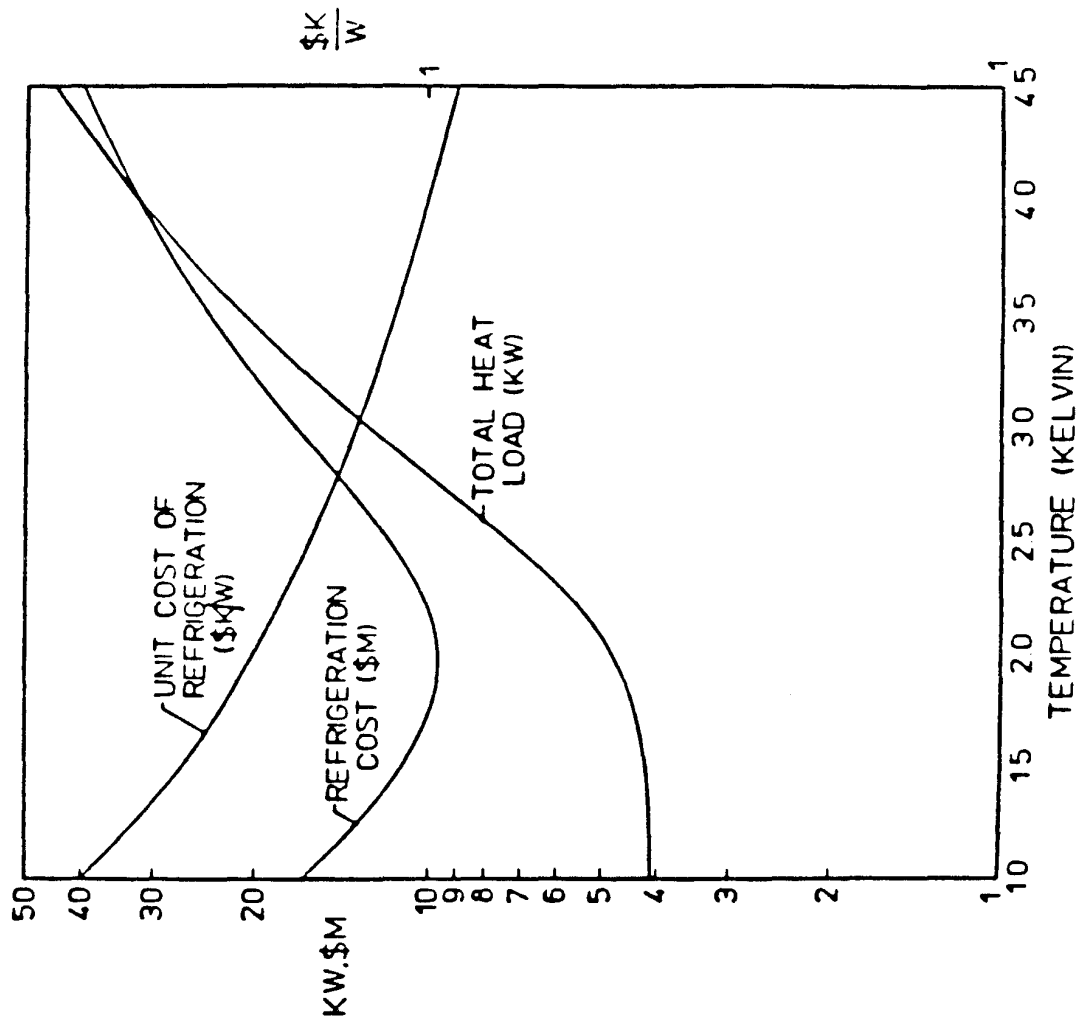

Figure 4. Schematic depiction of cost minimum resulting from heat load increasing and unit cost decreasing with increasing temperature.

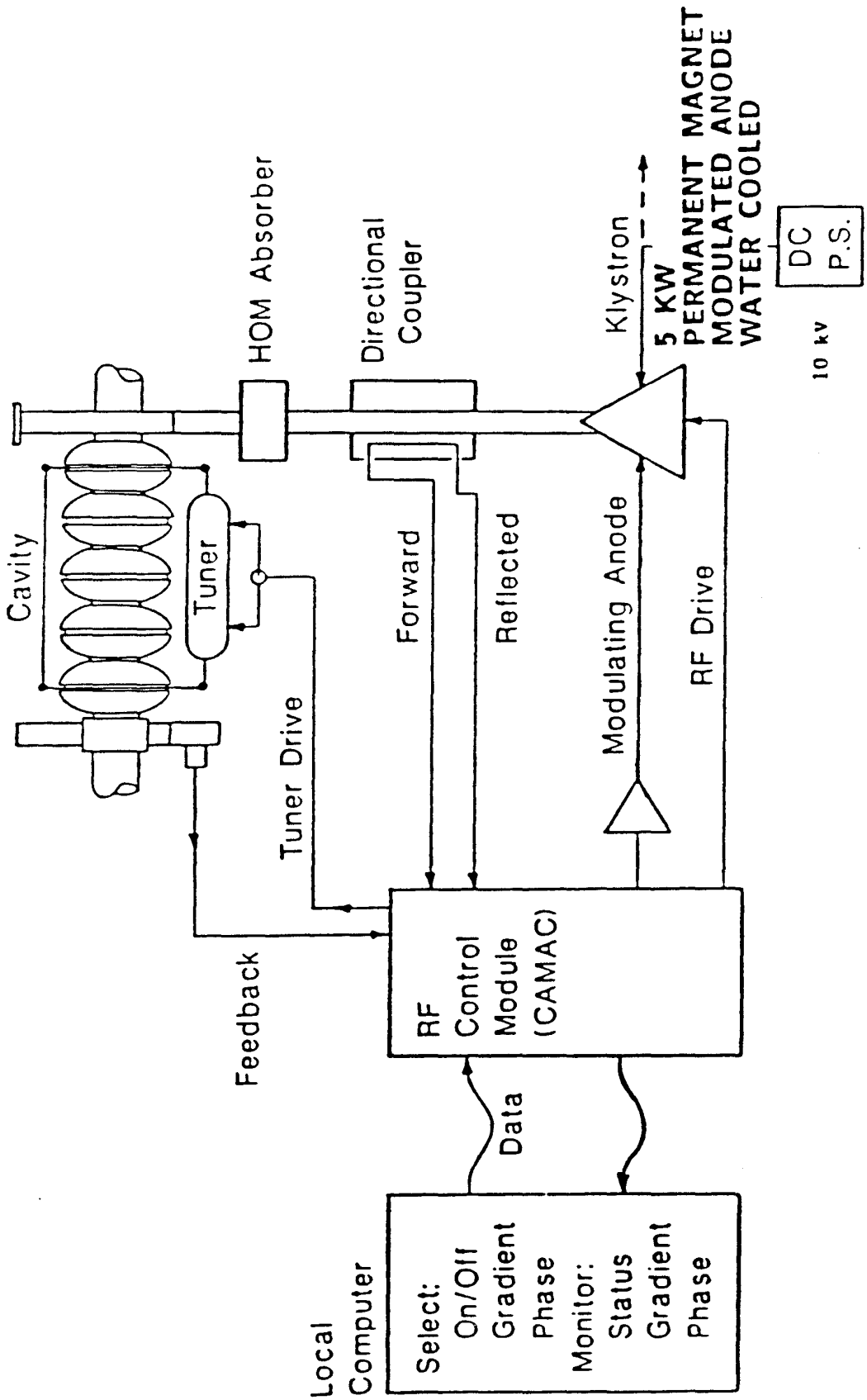

Figure 5. RF-system schematic.

within 1°, and the cavity field gradient is regulated to within 1 part in 10^4 by an rf control module. Continuously adjustable, modulo-360° phase shifters are used to generate the individual phase references, and a compensated rf detector is used for level feedback. The close-coupled digital system enhances system accuracy, provides self-calibration, and continuously checks the system for malfunction. Calibration curves, the operating program, and system history are stored in an on-board electrically erasable programmable read only memory (E^2PROM). The rf power is generated by a 5 kW, water-cooled permanent-magnet-focused klystron. The klystrons are clustered in groups of eight and powered from a common supply.

Energy spread and deviation of central energy from nominal operating value depend on control of bunch length from the injector, as well as of phase and amplitude of the accelerating field. With 400 cavities careful distinction between correlated and uncorrelated errors is necessary. It was found that some tolerances for the individual control modules can be reduced if a feedback loop for overall amplitude and phase, based on beam measurements in a high dispersion section of the lattice, is used. Requirements still remain stringent with maximum uncorrelated rms errors of a few 10^{-4} in voltage and at most a few degrees in phase. Correlated rms errors must be kept to below $2.2 \cdot 10^{-5}$ in amplitude and 0.24° in phase.

Figure 6 illustrates that over the entire planned current range, ~0 to 200 μA, gradients up to 10 MV/m can be achieved with 5 kW incident power. At the chosen Q_L of $\sim 6.6 \cdot 10^6$ a perfect match exists for 200 μA (through four passes) at 5 MV/m, and a good match at 10 MV/m; at lower current power is reflected. Current thinking is to place the klystron cavities at a VSWR minimum, but the use of circulators is still under investigation.

Beam Transport and Optics

Beam transport channels[16] can be classified into the beam switchyard (BSY), distributing beam to the end stations, and the accelerator internal transport elements. Looking at the latter, we can distinguish between the linac focusing structure and the seven recirculation half-arcs, four at the accelerator "east end," and three at the "west end."

The linac optics are set up as a simple FODO channel with half period length of 9.6 m with constant 120° phase advance along the full length of the first pass. Viewed from the linac, all east arcs are essentially "invisible," i.e., they represent isochronous, achromatic, identity transformations. On the second, and higher passes, focusing is weaker given the higher particle momentum, and phase advance per cell is no longer a constant. Therefore, there exists no longer a unique matched set of β-functions, and a continuum of input conditions results in a satisfactory beam envelope through the linac. Correspondingly, the west arcs are tuned to more general transformations in the transverse phase space while retaining the features of isochronicity and achromaticity.

The structure of each arc arises from five distinct regions: spreaders, matching/extraction region, arcs proper, matching region, and recombiners. Spreaders and recombiners are achromatic, vertical, double bends. Originally conceived as

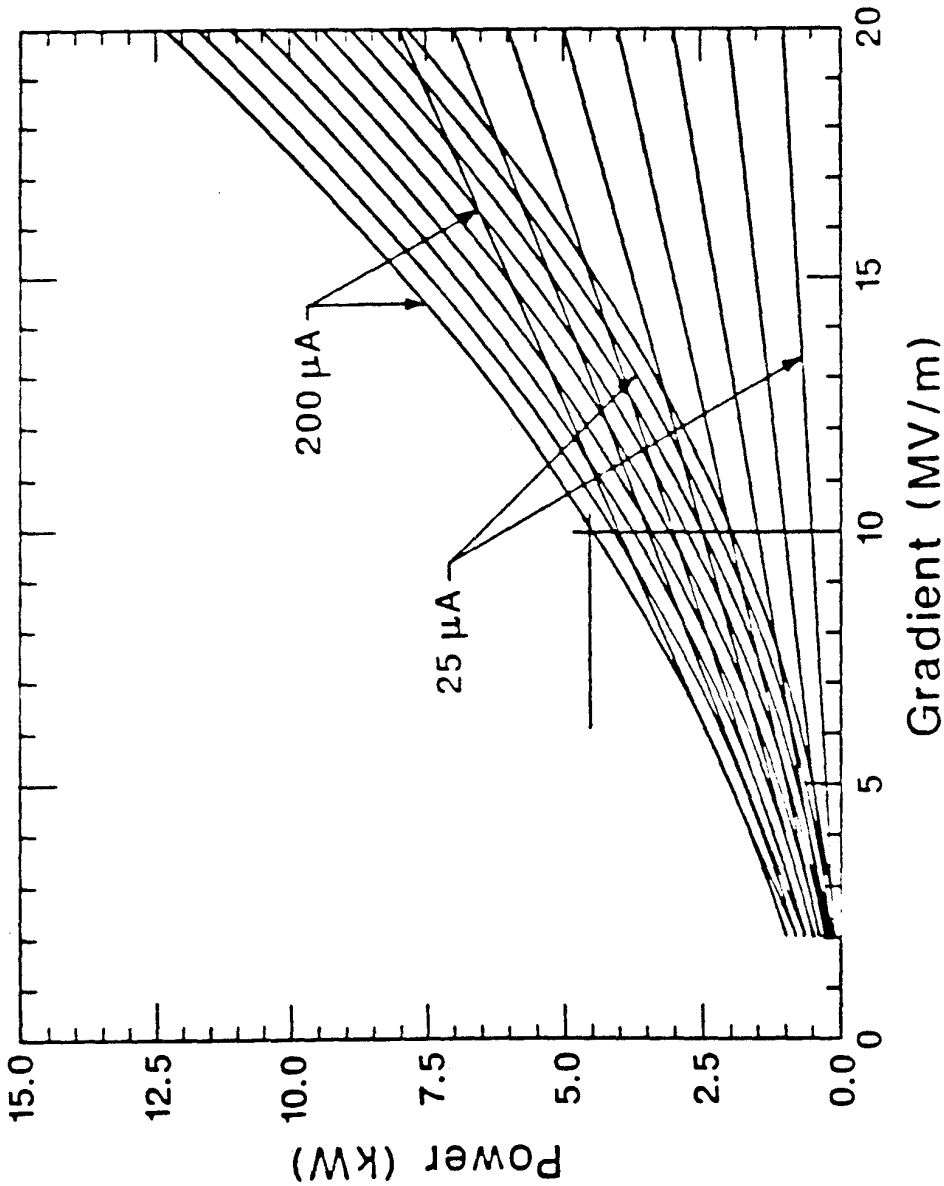

Figure 6. Incident power required versus cavity gradient for $Q_z = 6.6\text{-}10.^6$ and currents from 0 to 200 μA (curved lines). Straight lines represent power going into beam.

(α, $-\alpha$) layouts, the presently adopted version executes the vertical displacement in a staircase fashion (Fig. 7). This results in weaker quadrupoles to achieve achromaticity as well as lower β-functions, which together reduce sensitivity to quad alignment errors and vibrations by nearly one order of magnitude. Matching and matching/extraction sections are straight sections containing quadrupoles to match β-functions into (or from) the arcs proper from the spreaders (or into the recombiners). Path length adjusting "dog legs" are located in the matching/extraction regions, and extraction gear is installed in the west region with the east region remaining for future expansion at a later time.

The arcs proper, isochronous and achromatic, are based upon the second order achromat principle, made up of a periodic array of cells, synchrotron lattice fashion. Lower-energy arcs contain fewer dipoles, but have essentially the same focusing structure. Recent refinements have led to vertical stacking of all arcs with key elements occupying identical, or almost identical, horizontal locations.

Issues, R&D, and Construction Progress

Key Issues and Challenges

Three categories stand out:

- the technological feasibility—the question of reliable large-scale application of rf superconductivity—particularly in the context of a "green site" laboratory and project,
- the beam dynamics feasibility, where the outstanding questions pertain to beam stability and beam quality,
- operability: the issues pertaining to effective commissioning of this highly complex machine.

The technological issues are addressed in a three-prong approach. First, the formation of a strong SRF Technology Division at CEBAF, including key members of and replacing since July 1, 1987, the formal Cornell collaboration; second, the buildup of a well-equipped test lab that will serve advanced R&D, support machine operation and maintenance, and most importantly support construction by providing processing, testing, and assembly capability, as well as some level of fabrication capability; and third, an aggressive industrial prototyping program for cavities and cryostats.

Figures 8 and 9, showing test results for single cavities as well as cavity pairs, show that expectations have been exceeded by far, with respect to both gradient and Q values, with the exception of a single cavity that had a lower Q value due to a well understood and acknowledged processing mistake. All components for a full cryomodule (i.e., an eight-cavity cryostat made up of four subassemblies, cryounits, each containing two cavities) have been delivered. A first cryounit is presently undergoing initial cryogenic tests at CEBAF. Tests of a four-cavity subcryomodule are expected to be completed in May 1988. In the course of this program a number

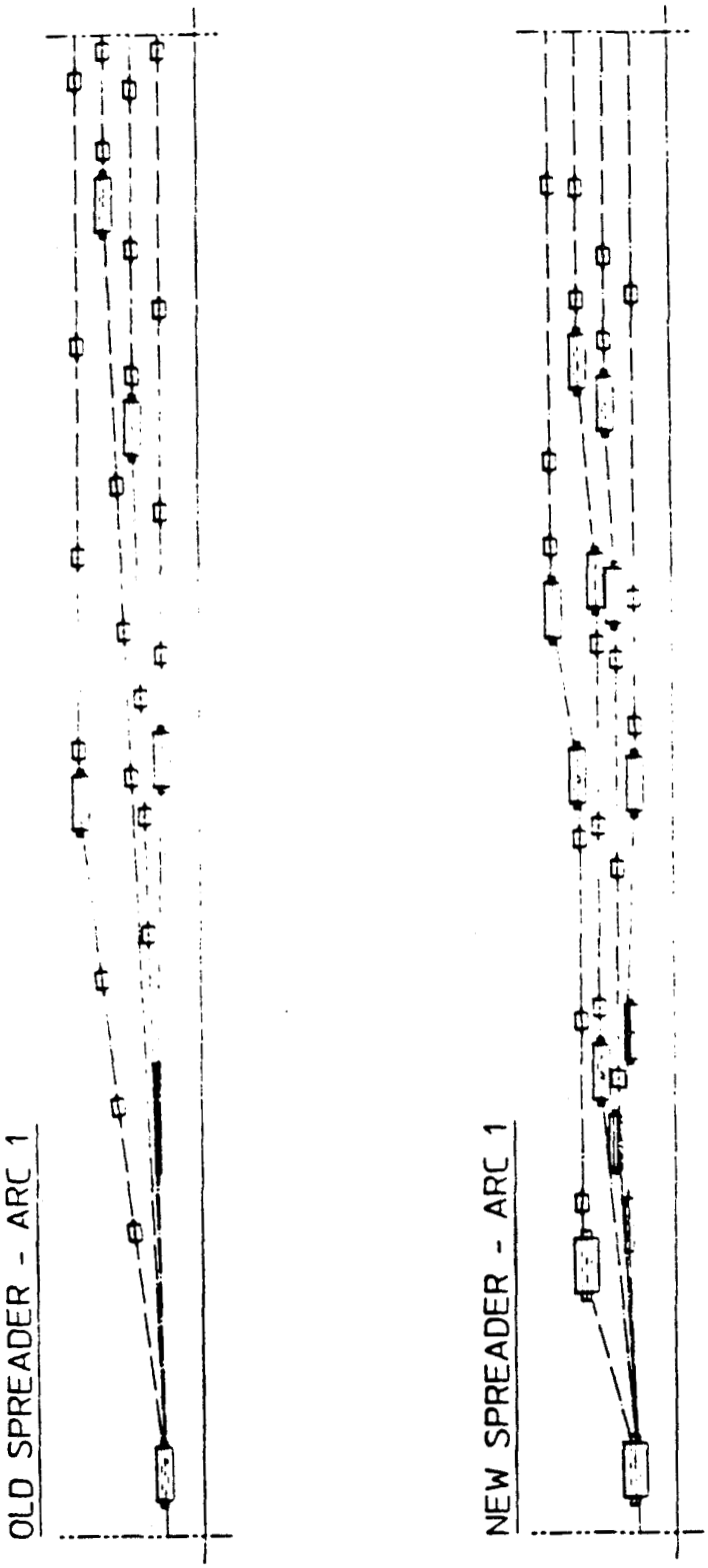

Figure 7. Layout of spreader region. Lower figure shows "staircase" design that achieves achromaticity with weaker triplet, and exhibits less error sensitivity.

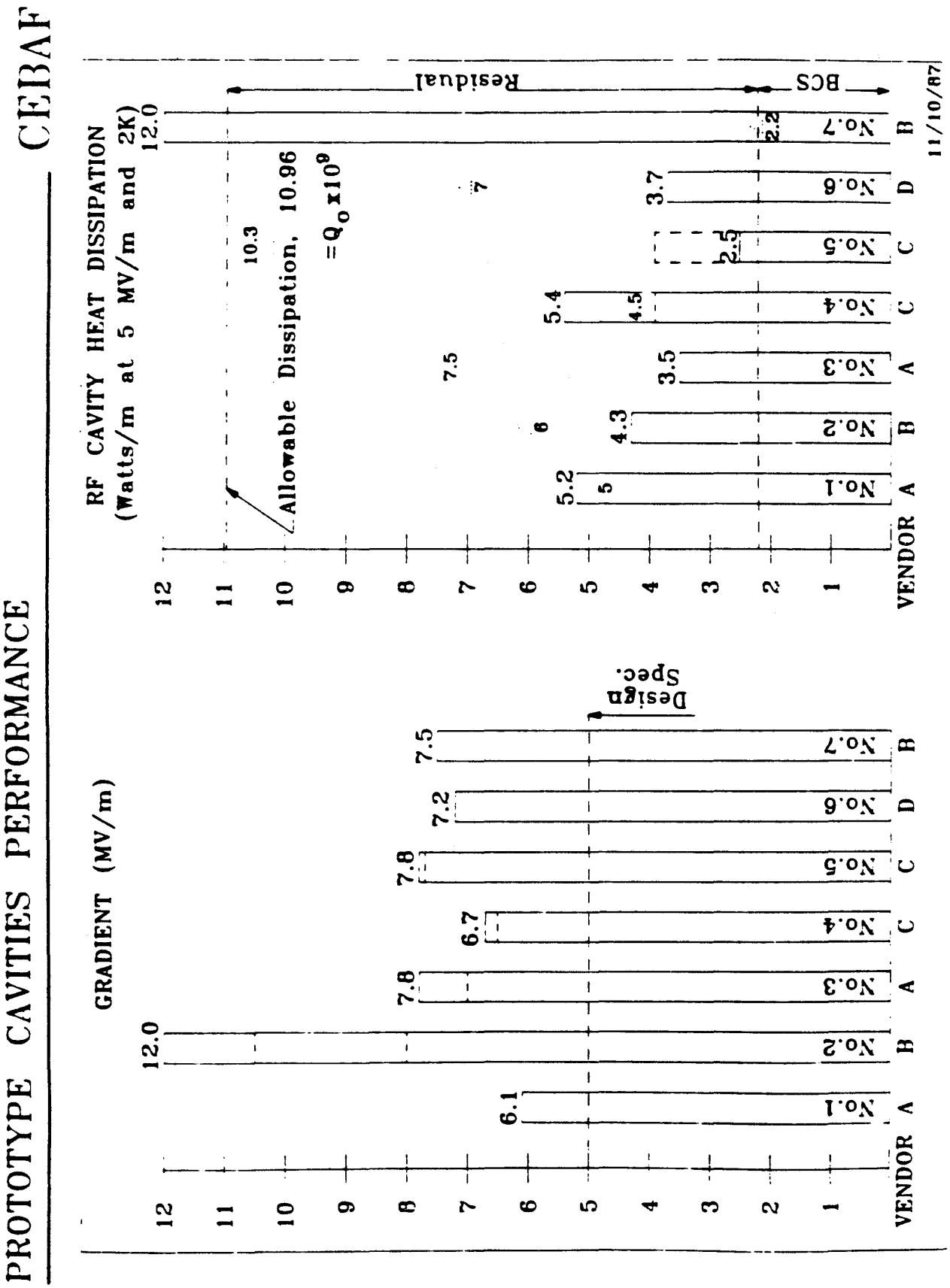

Figure 8. Prototype cavity test results.

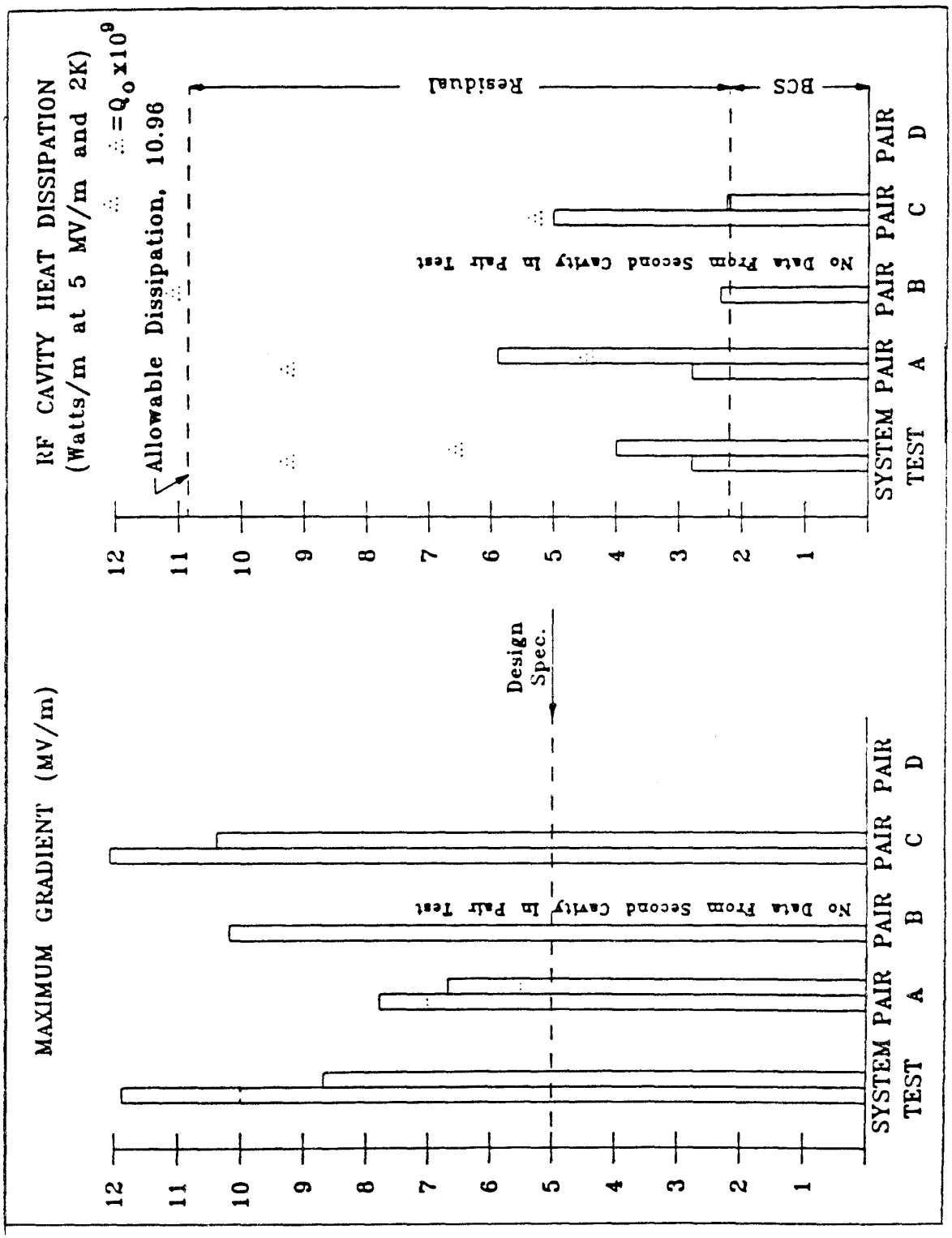

Figure 9. Prototype cavity pair test results.

of highly desirable changes in cryostat design have been identified that include increased clearances for cavity insertion, flexible bellows at the rf feedthrough plate, improved cavity-support and He vessel-alignment structures, and welded bridging components in the outer vacuum wall. All these changes are viewed as straightforward and highly desirable engineering tasks that will greatly facilitate assembly in production. A full first cryounit of the new design will be tested in August 1988, and a full cryomodule containing eight cavities will have its tests completed in March 1989. Although this represents a delay compared to previous R&D plan objectives, the insight and understanding gained are thorough, and the procurement plan for the construction project is structured in such a way that no overall project delays are expected.

Beam dynamics feasibility means primarily beam stability but also the capability to maintain beam quality under the action of a number of potentially quality-degrading mechanisms. The most important of these phenomena is the electromagnetic interaction between the beam and the "wall," i.e., the conducting boundary formed by cavities, beam position monitors, and the vacuum pipe. We can distinguish multi-bunch and single bunch phenomena, and furthermore categorize into single and multipass phenomena. Typically the distinction between single pass and multipass is blurred or disappears for phenomena of interest in the case of intense, widely spaced bunches. For CEBAF the critically important phenomenon is multi-bunch, multipass BBU.

Two codes have been developed to analyze beam behavior, a 2D simulation[17] code and a 1D "analytical"[18] code based on matrix techniques. Both codes allow the use of realistic lattices as well as HOM frequency distributions and yield excellent agreement between them with regard to prediction of threshold current. This is found to exceed design currents by two orders of magnitude. The 2D simulation also allows study of subthreshold emittance degradation, an effect found unimportant at the few hundred μA level. Figure 10 shows results of these computations. More detail is to be found in another contribution to this workshop.[19]

An apparent emittance degradation can occur through coupling between longitudinal and transverse phase planes, i.e., differential steering from bunch head to bunch tail. This occurs at the power couplers in the accelerating cavities where the accelerating field varies across the aperture, and by necessity also in the rf separators. The cure consists in the adopted "left-right-right-left" arrangement of cavity power couplers and in the choice of the lowest practical frequency for the rf separators.

The increase in momentum spread and emittance has been previously mentioned. Synchrotron radiation introduces a momentum spread, $\sigma_E^2 \propto \gamma^7/\rho^2$, where γ has its usual relativistic meaning and ρ is the magnetic bend radius, and an emittance increase, $\Delta\epsilon \propto \gamma^5\langle\mathcal{H}\rangle/\rho^2$, where $\langle\mathcal{H}\rangle$ is a measure of relevant lattice properties. σ_E and $\Delta\epsilon$ are controlled by generous radii ρ, and strong focusing leading to a small value of $\langle\mathcal{H}\rangle$.

Operability is an area deserving early attention because CEBAF is a relatively complex device. It contains over 1800 magnets, more than half of which are on

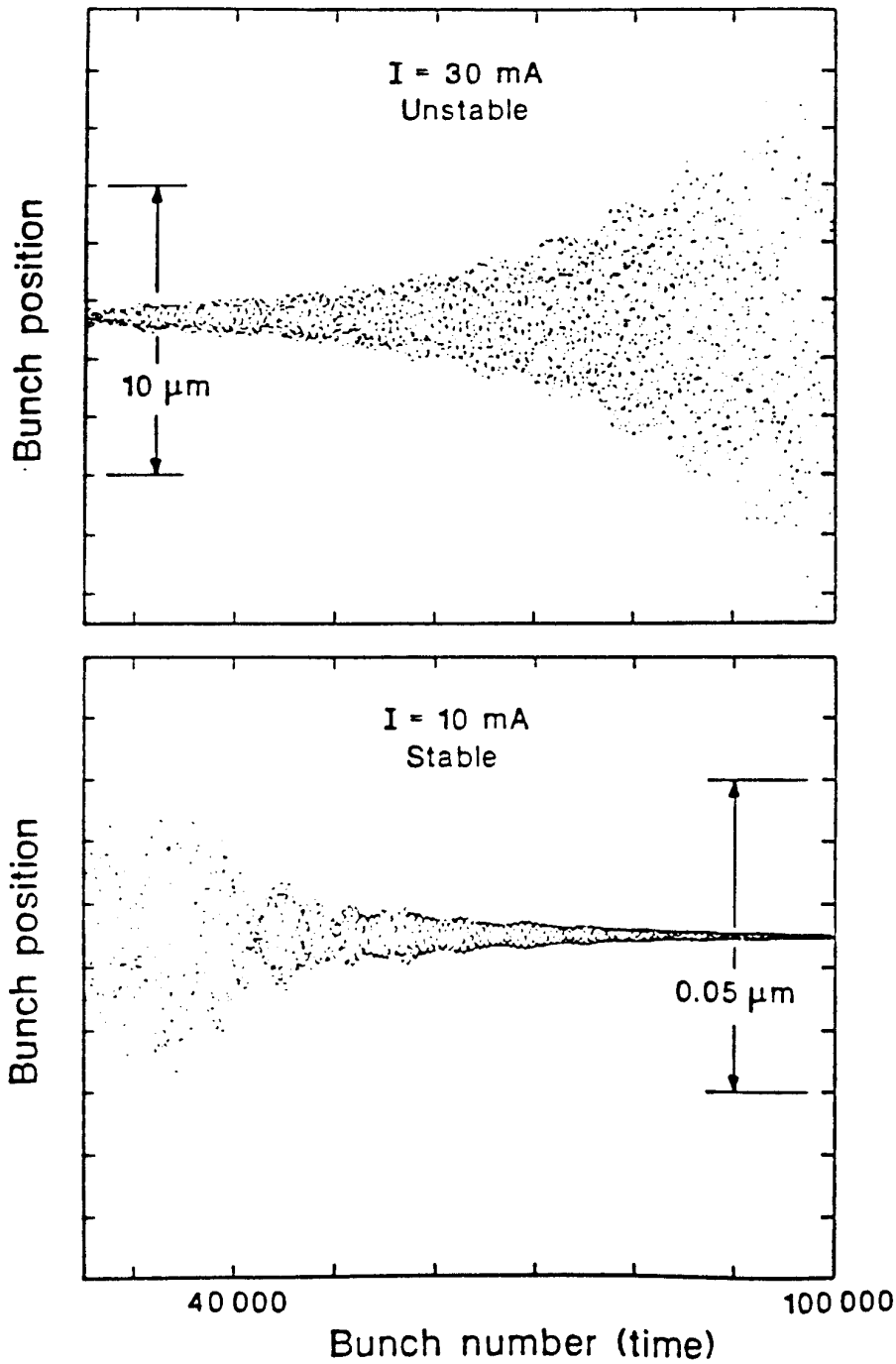

Figure 10. Simulation results clearly show instability for an average current of 30 mA and stability for 10 mA. Bunches are injected off-axis, thereby exciting deflecting modes. Shown is their centroid transverse position leaving the linac after four passes, plotted vs. bunch number, i.e., time.

individual circuits; the quadrupoles, steering dipoles, and beam position monitors number over 500 each, and the total beam path length is ~5 km with a total phase advance of ~120 π in betatron space. Combined with a severely beam-loaded rf system requiring very precise control, this calls for early attention to operational aspects, issues, and procedures. Early commissioning (e.g., front end test for 50 MeV in 1990) and extensive computer modeling are key ingredients in our approach. Elements in facilitating commissioning and operations are a very powerful computer control system and a deliberate design philosophy of "functional modularity," i.e., an attempt to maximize one-to-one correspondence between certain components and particular actions on the beam as exemplified in the arc design.

Recent Accomplishments and Outlook

Preconstruction R&D is actively going on in areas such as magnets, magnet measurement, injector and rf separator development, beam diagnostics and computer modeling. A first electron beam at 80 keV has been produced, a beam position monitor has been bench tested, and an initial rf separator design has been prepared and calculated. An initial version of an accelerator computer model is in place, and extensive calculations, numerical and analytical, have established an initial impedance catalog for the full frequency range applicable to CEBAF's short bunches, i.e., over several hundred GHz, far beyond pipe cutoff.

Experimental end station conventional facilities layout will be finalized in spring 1988 and conceptual designs for the equipment submitted in fall 1988.

Site clearing and preparation are complete; tunnel civil construction will begin in 1988. The contract for the central helium liquifier is about to be placed, and cavity procurement will commence in 1988. First 45 MeV beam is expected in 1990. Preoperations and subsystem commissioning will start in 1989 and continue at increasing effort level through 1992. Commissioning of the full accelerator facility will begin in 1993.

References

[1] Report of the NSAC ad hoc Subcommittee on a 4 GeV CW Electron Accelerator for Nuclear Physics, September 1984.

[2] Future of Nuclear Science, NAS 1977, Friedlander Panel, National Research Council, National Academy of Science, 1977.

[3] Long Range Plan for Nuclear Science, DOE/NSF Nuclear Science Advisory Committee, 1979.

[4] The Role of Electron Accelerators in US Medium Energy Nuclear Science, ORNL/PPA-77/4, 1977.

[5] The Role of Electromagnetic Interaction in Nuclear Science, DOE/NSF Nuclear Science Advisory Committee, 1983.

[6] Long Range Plan for Nuclear Science, DOE/NSF Nuclear Science Advisory Committee, 1983.

[7] A Report of the Panel on Electron Accelerator Facilities, DOE/NSF Nuclear Science Advisory Committee, 1983.

[8] CEBAF Pre-construction Technology Review, 1985.

[9] Scientific and Technological Assessment Report (STAR), CEBAF, Nov. 1985.

[10] Preliminary Conceptual Design Report (PCDR), CEBAF, Nov. 1985.

[11] Conceptual Design Report (CDR), CEBAF, Feb. 1986.

[12] Ronald M. Sundelin, High Gradient Superconducting Cavities for Storage Rings, IEEE Trans. Nuclear Science NS-32, No. 5, (1985) pp. 3570—3573.

[13] M. Wilson et al, NBS-LANL RTM Injector Installation, IEEE Trans. Nuclear Science NS-30, No. 4 (1983), p. 3021.

[14] Nuclear Physics with a 450 MeV Cascade Microtron, University of Illinois Nuclear Physics Laboratory Report, March 1986.

[15] W. Diamond, The Injector for the CEBAF CW Superconducting Linac, in 1987 Particle Accelerator Conference Proceedings.

[16] R. C. York and D. R. Douglas, Optics of the CEBAF CW Superconducting Accelerator, in 1987 Particle Accelerator Conference Proceedings.

[17] J. J. Bisognano and G. A. Krafft, Multipass Beam Breakup in the CEBAF Superconducting Linac, in 1986 Linear Accelerator Conference Proceedings, pp. 452—454.

[18] G. A. Krafft and J. J. Bisognano, Two-Dimensional Simulations of Multipass Beam Breakup, in 1987 Particle Accelerator Conference Proceedings.

[19] Superconducting RF and Beam-Cavity Interactions, J. J. Bisognano, These Proceedings.